The Competitive Adsorption of Chromate and Sulfate on Magnetite Surface: An ATR-FTIR Study

Xiaoju Lin [1,2,3,4], **Gaoling Wei** [5], **Xiaoliang Liang** [1,2,3,4,*], **Jing Liu** [1,2], **Lingya Ma** [1,2,3,4] and **Jianxi Zhu** [1,2,3,4]

[1] CAS Key Laboratory of Mineralogy and Metallogeny/Guangdong Provincial Key Laboratory of Mineral Physics and Material Research & Development, Guangzhou Institute of Geochemistry, Chinese Academy of Sciences, Guangzhou 510640, China; linxiaoju@gig.ac.cn (X.L.); liujing187@gig.ac.cn (J.L.); ma-lingya@gig.ac.cn (L.M.); zhujx@gig.ac.cn (J.Z.)

[2] CAS Center for Excellence in Deep Earth Science, Guangzhou, 510640, China.

[3] University of Chinese Academy of Sciences, Beijing 100049, China.

[4] Institutions of Earth Science, Chinese Academy of Sciences, Beijing 100029, China.

[5] National-Regional Joint Engineering Research Center for Soil Pollution Control and Remediation in South China, Guangdong Key Laboratory of Integrated Agro-environmental Pollution Control and Management, Institute of Eco-environmental and Soil Sciences, Guangdong Academy of Sciences, Guangzhou 510650, China; gaoling_wei@126.com

[*] Correspondence: liangxl@gig.ac.cn

Text. S1. Preparation Procedure of Ni-Containing Magnetite by a Precipitation–Oxidation Method.

All chemicals and reagents used in this work were of analytical grade and used as received. $FeSO_4 \cdot 7H_2O$ (0.60 mol·L^{-1}) and $NiCl_2 \cdot 6H_2O$ (0.30 mol·L^{-1}) were dissolved in 400 mL of HCl solution. Hydrazine (1.0 mL) was added to prevent the oxidation of Fe^{2+} cations, and the pH was low enough (<1) to prevent Fe^{2+} oxidation and hydroxide precipitation. This solution was heated to 90–100 °C. Equal volumes of a solution containing 4.0 mol·L^{-1} NaOH and 0.90 mol·L^{-1} $NaNO_3$ were added dropwise (10 mL·min^{-1}) into the heated iron solution, and the reaction was maintained at 90 °C for 2 h while stirring at a rate of 500 rpm. Then, the solution was cooled to room temperature. It is necessary to emphasize that, during the reaction, N_2 was passed through to prevent the oxidation of Fe^{2+} by air. The particles were then separated by centrifugation at 3500 rpm for 5 min and washed with boiling distilled water, followed by additional centrifugation. After 3–4 washings, the particles were collected and dried in a vacuum oven at 100 °C for 24 h. The samples were ground and passed through a 200-mesh screen. The contents of Fe and Ni were determined spectrophotometrically by the phenanthroline and dimethyglyoxime methods. The molar ratio of Ni/Fe was 0.456.

Text. S2. Analysis of ATR-FTIR Spectra by Using the 2D-COS Technique.

To obtain an accurate assignment of the IR peaks for the surface complexes, the spectra were analyzed using the 2D-COS technique. The original spectra, after baseline correction, smoothing and calculation, were transferred to the 2D correlation spectra, including synchronous $\Phi(\nu_1, \nu_2)$ and asynchronous $\psi(\nu_1, \nu_2)$ contour plots, using the 2D Shige Program ver. 1.3 (Shigeaki Morita, Kwansei-Gakuin University, Hyogo, Tokyo, 2004–2005). The intensity of the synchronous 2D correlation spectrum $\Phi(\nu_1, \nu_2)$ represents the simultaneous changes of two separate bands at ν_1 and ν_2. In the synchronous spectrum, an auto-peak located at a diagonal position indicates the change of one peak intensity with time. Cross peaks located at off-diagonal positions show the response to simultaneous changes in spectral intensities observed at two different bands at ν_1 and ν_2. The intensity of an asynchronous 2D correlation spectrum $\psi(\nu_1, \nu_2)$ represents sequential (or not simultaneous) changes of two bands at ν_1 and ν_2. The asynchronous spectrum is a powerful tool for resolving overlapping peaks and enhancing spectral resolution. In an asynchronous spectrum, only cross peaks can be found, indicating the uncorrelated response of two bands likely originating from different surface complexes. ν_1 and ν_2 change simultaneously if $\psi(\nu_1, \nu_2)$ is zero, which indicates that they belong to the same adsorption complexes. Otherwise, they display uncorrelated responses and belong to different adsorption complexes.

Table S1. A synchronous relationship of peaks on the synchronous ($\Phi(\upsilon_1, \upsilon_2)$) and asynchronous spectra ($\psi(\upsilon_1, \upsilon_2)$) of chromate adsorbed on the magnetite surface.

Wavenumber/cm^{-1}	950	930	910	890	870	830	820
950			√		√		
930			√			√	
910				√	◎	◎	√
890					√		
870							
830							
820							

◎: the synchronous correlation of cross peak $\Phi(\upsilon_1, \upsilon_2)$. √: the asynchronous correlation of cross peak $\psi(\upsilon_1, \upsilon_2)$.

Table s2. A synchronous relationship of peaks on the asynchronous spectra of sulfate adsorbed on the magnetite surface.

Wavenumber/cm^{-1}	1135	1106	1058	976
1135		√		
1106			√	√
1058				
976				

√: the asynchronous correlation of cross peak $\psi(\upsilon_1, \upsilon_2)$.

Figure S1. XRD pattern of as-prepared Ni-containing magnetite.

Power X-ray diffraction (PXRD) was recorded between 10° and 80° (2θ) at a step of 1° min^{-1} using a Bruker D8 advance diffractometer with Cu Kα radiation (40 kV and 40 mA). Seven narrow sharp peaks could be obviously observed, indicating the (111), (220), (311), (400), (422), (511) and (440) planes of Ni-doped Fe_3O_4 (JCPDS card no.190629). The XRD pattern of Ni-containing magnetite corresponds well to the standard card of magnetite (JCPDS: 19-0629), confirming that the as-prepared sample was composed of Ni-doped Fe_3O_4.
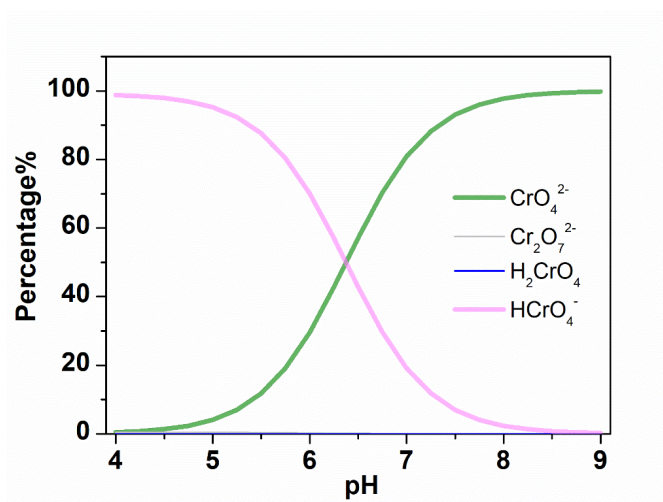
Figure S2. Contribution of aqueous species of chromate at different pH values calculated by the Visual MINTEQ program.
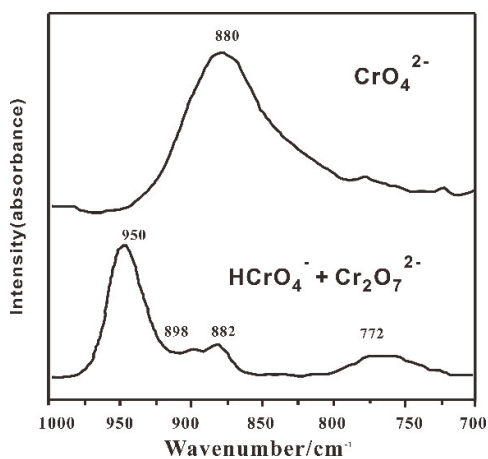

Figure S3. ATR-FTIR spectra of aqueous chromate (100 mmol·L⁻¹) at pH 10 (top) and pH 3 (bottom) [1].
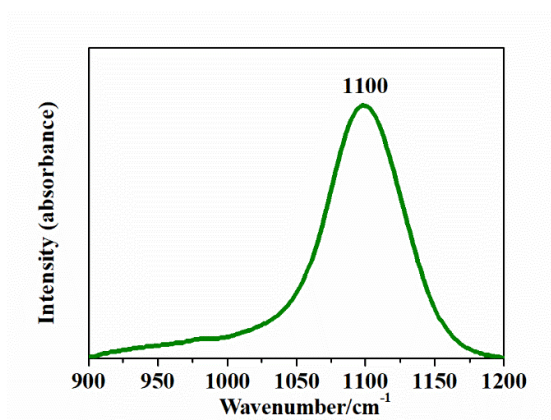

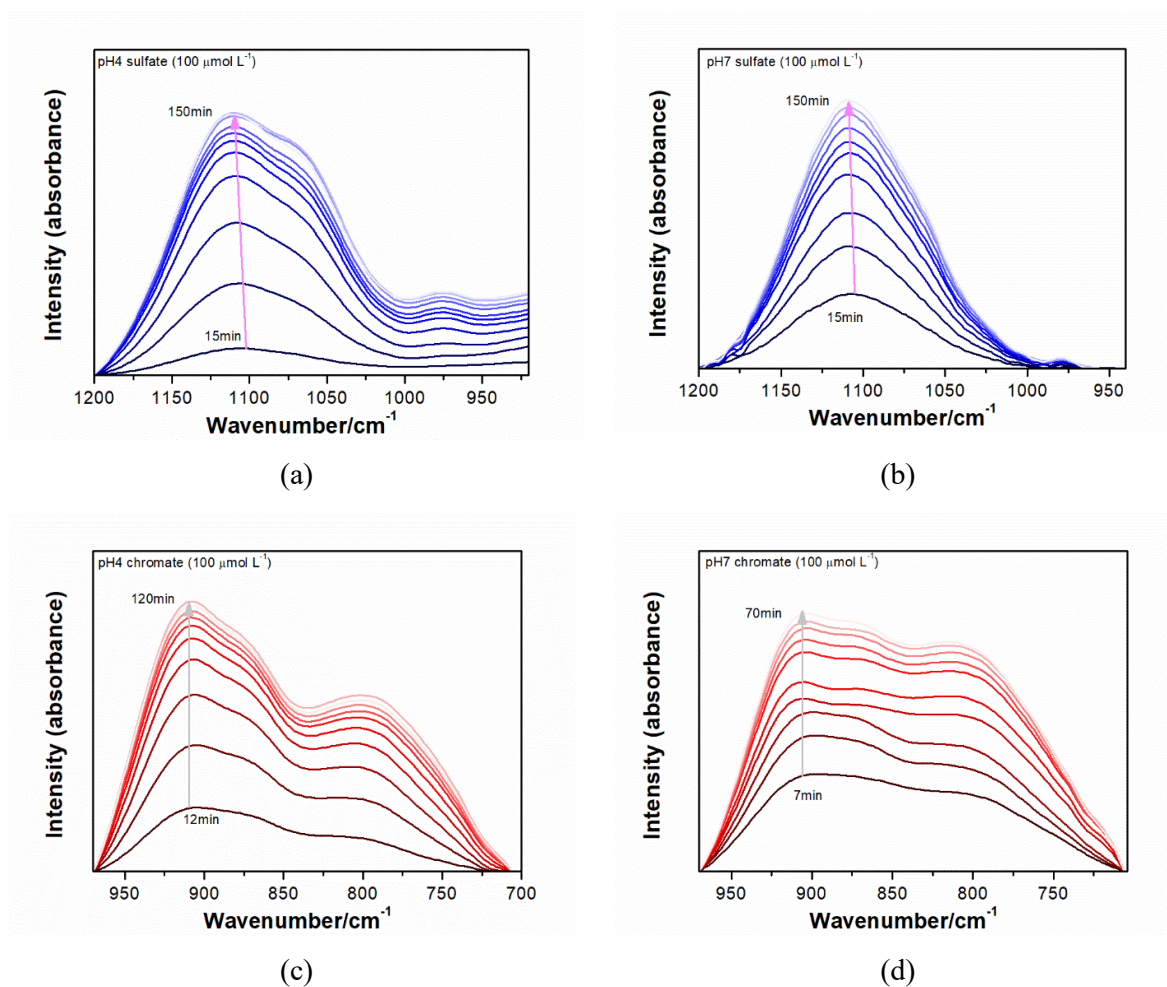**Figure S4.** ATR-FTIR spectra of aqueous sulfate (10 mmol·L⁻¹) at pH 8.

(a)

(b)

(c)

(d)

Figure S5. Pre-adsorption of chromate (**a, b**) or sulfate (**c, d**) on Ni-substituted magnetite at pH 4 and pH7.
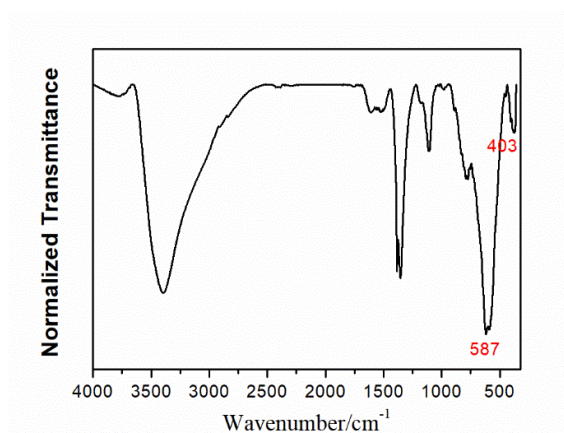

Figure S6. IR spectra of Ni-substituted magnetite.

The FTIR spectra were also applied to distinguish the magnetite and maghemite. Figure S6 showed characteristic bands at 587 cm^{-1} and 403 cm^{-1} which are due to the Fe–O band in tetrahedral and octahedral sites. It was different with the characteristic Fe–O band at 552 cm^{-1} of maghemite [2], verifying the sample phase of magnetite.
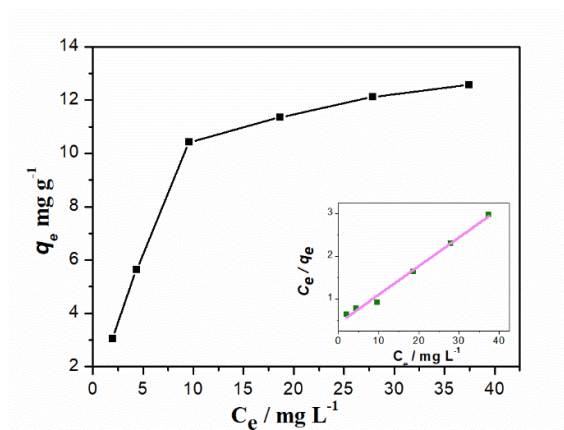
Figure S7. The Cr(VI) adsorption isotherms of Ni-substituted magnetite.

Figure S7 shows the adsorption isotherms of the adsorption of Cr(VI) onto Ni-substituted magnetite at pH5. The Langmuir equation was used to describe the Cr(VI) adsorption. The linear form of the Langmuir plot is given as $C_e/q_e = 1/(bQ_m) + (1/Q_m)C_e$, where Q_m (mg·g^{-1}) is the adsorption capacity. In this study, the adsorption capacity of Cr(VI) on Ni-substituted magnetite is 15 mg·g^{-1}, which is similar to that of pure magnetite [3,4].
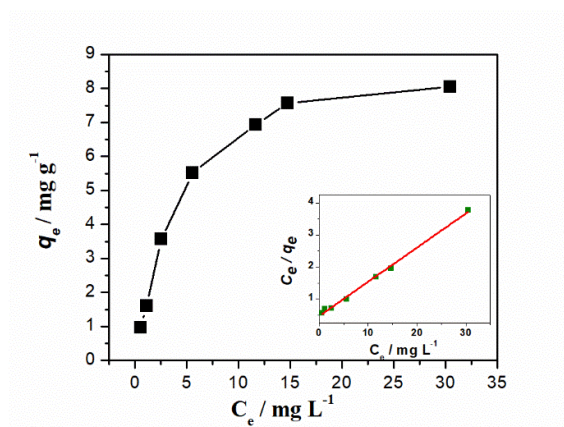

Figure S8. The S (VI) adsorption isotherms of Ni-substituted magnetite.

Figure S8 shows the adsorption isotherms of the adsorption of Cr(VI) onto Ni-substituted magnetite at pH5. The Langmuir equation was used to describe the S(VI) adsorption. The linear form of the Langmuir plot is given as $C_e/q_e = 1/(bQ_m) + (1/Q_m)C_e$, where Q_m (mg·g^{-1}) is the adsorption capacity. In this study, the adsorption capacity of S(VI) on Ni-substituted magnetite is 9.3 mg·g^{-1} [5,6].